INSTITUTE OF PHYSICS PUBLISHING JOURNAL OF PHYSICS D: APPLIED PHYSICS

J. Phys. D: Appl. Phys. **39** (2006) 2890–2896 doi:10.1088/0022-3727/39/14/003

The effects of applied magnetic fields on the α/γ phase boundary in the Fe–Si system

M C Gao[1,3] T A Bennett[1], A D Rollett[1] and D E Laughlin[1,2]

[1]Department of Materials Science and Engineering, Carnegie Mellon University, Pittsburgh, PA 15213, USA

[2]Data Storage Systems Center, Carnegie Mellon University, Pittsburgh, PA 15213, USA

E-mail: mgao05@yahoo.com

Received 18 February 2006, in final form 23 May 2006
Published 30 June 2006
Online at stacks.iop.org/JPhysD/39/2890

Abstract

The CALPHAD (calculations of phase diagrams) method is used to examine the effects of applied magnetic fields on the α/γ phase boundary in the Fe–Si system in the paramagnetic state. The reported susceptibility data for pure Fe is first re-evaluated. The contributions to the total Gibbs energy of the ferrite (α) and austenite (γ) from the external fields are calculated based on the Curie–Weiss law and the re-evaluated susceptibility data. The Fe–Si phase diagram on the Fe-rich side as a function of applied field is calculated using the Thermo-Calc™ package. With increasing field strength, the γ loop shrinks monotonically; that is, the α/γ-Fe transition temperature increases while that for γ/δ-Fe transition decreases, albeit more slowly. Finally, in conformance with the existing CALPHAD databank, Redlich–Kister polynomials are proposed to account for the compositional and temperature dependence of the contribution to the total Gibbs energy from the applied field in the paramagnetic state in the range over which the Curie–Weiss law is obeyed.

1. Introduction

Modification of thermo-mechanical processing by magnetic fields has been growing substantially in the last decade [1–20]. The goal of such processing is to achieve superior material properties that cannot be obtained through the more conventional thermo-mechanical treatments. This is possible because strong magnetic fields can significantly change the phase stability, phase boundaries [1, 4, 5–9, 12, 13, 15, 19 , 20] and also phase transformation kinetics [14, 19, 20], where the phases involved exhibit different magnetization responses. A variety of theoretical approaches have been taken to study the effect of external magnetic fields on phase transformations [1, 3, 8–10, 12, 13, 15], but a systematic approach that uses computational phase diagram predictions under the influence of applied fields has not yet been reported. The present authors are studying the effect of applied magnetic fields on the recrystallization and grain growth behaviour in Fe-1Si (in wt%) alloy [18], and they believe that magnetization (due to internal magnetic state and external applied magnetic field) plays an important role in solute segregation at grain boundaries (GB) and therefore grain growth kinetics. Since solute segregation is closely related to bulk thermodynamics, investigation of the effect of external magnetic fields on the bulk thermodynamics is evidently appropriate.

It is well known that Si is a very strong bcc (α) stabilizer since alloying Fe with Si decreases the Gibbs energy of the α phase (mainly through the enthalpy) much more significantly than it does that of the γ phase. As a result, a closed γ loop is observed in the temperature-composition phase diagram, as shown in figure 1. The region of the two-phase field between the α and γ phases spans a very narrow composition range because the Gibbs energy-composition curves of (solid solution) α and γ phases in the Fe–Si system are similar in that region (see figure 2). In relation to the Fe-1Si composition, it is sufficient to focus on the γ loop in order to evaluate the effect of an applied magnetic field. Pure bcc-Fe is ferromagnetic with a Curie temperature of ~770 °C which drops rapidly

[3] Author to whom any correspondence should be addressed.

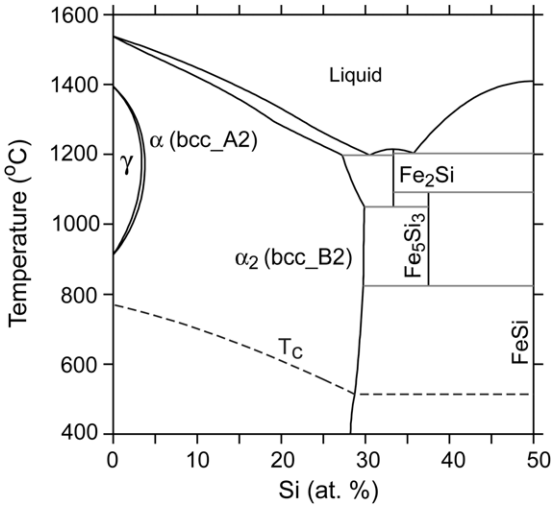

Figure 1. Calculated Fe-rich Fe–Si phase diagram without external magnetic field, using the thermodynamic descriptions from [35]. Dashed line separates the disordered bcc-A2 and ordered bcc-B2 phase. Dotted line shows the calculated ferromagnetic Curie temperature.

with increasing Si content. Pure fcc-Fe is paramagnetic in the temperature ranges within which it is stable. Since the γ loop ($\geqslant$912 °C and Si $\leqslant$4 at.%) involves temperatures that are well above the Curie temperature of α, the current investigation focuses on the paramagnetic behaviour of both the α and γ phases under an applied external magnetic field and its effect on the loop. However, the method adopted can be applied in principle to other paramagnetic systems where the Curie–Weiss law is obeyed. Since the magnetic susceptibility of the α phase is much larger than that of the γ phase, it is reasonable that the γ loop shrinks progressively with increasing applied field strength, since the Gibbs energy of the α phase is lowered more than that of the γ phase by applied magnetic fields.

Polymorphic transitions in pure Fe and in the Fe–C system were previously investigated by Guo and Enomoto [8, 9], Hao and Ohtsuka [12] and Joo *et al* [13]. These studies used the Weiss molecular field (WMF) theory together with the Curie–Weiss law to evaluate the change in Gibbs energy of the individual phases involved and calculate an equilibrium phase diagram especially Fe–C and Fe–C-TM (TM signifies transition metals) with applied magnetic fields. Not surprisingly, their results appear to be similar since the same methodologies and the same susceptibility data were used. A commonly accepted estimate on the effect of magnetic field is that the phase boundaries change by about 1 °C T^{-1} of applied field [15]. Hao and Ohtsuka [12] reported a value 0.8 °C T^{-1} for the phase boundary between bcc and fcc of pure Fe in the paramagnetic state when the applied filed is low ($\leqslant$10 T). In this report, the paramagnetic susceptibility data of pure Fe in its bcc and fcc structures [21–27] is first re-evaluated. The new susceptibility values as a function of temperature are then used to calculate the Gibbs energy change due to applied magnetic fields based upon the Curie–Weiss law. The change in Gibbs energy as a function of temperature, while holding the field strength constant, is inserted into the CALPHAD database. Finally, Thermo-Calc^{TM} [28] was used to calculate new Fe–Si equilibrium phase diagrams under the influence of an applied magnetic field.

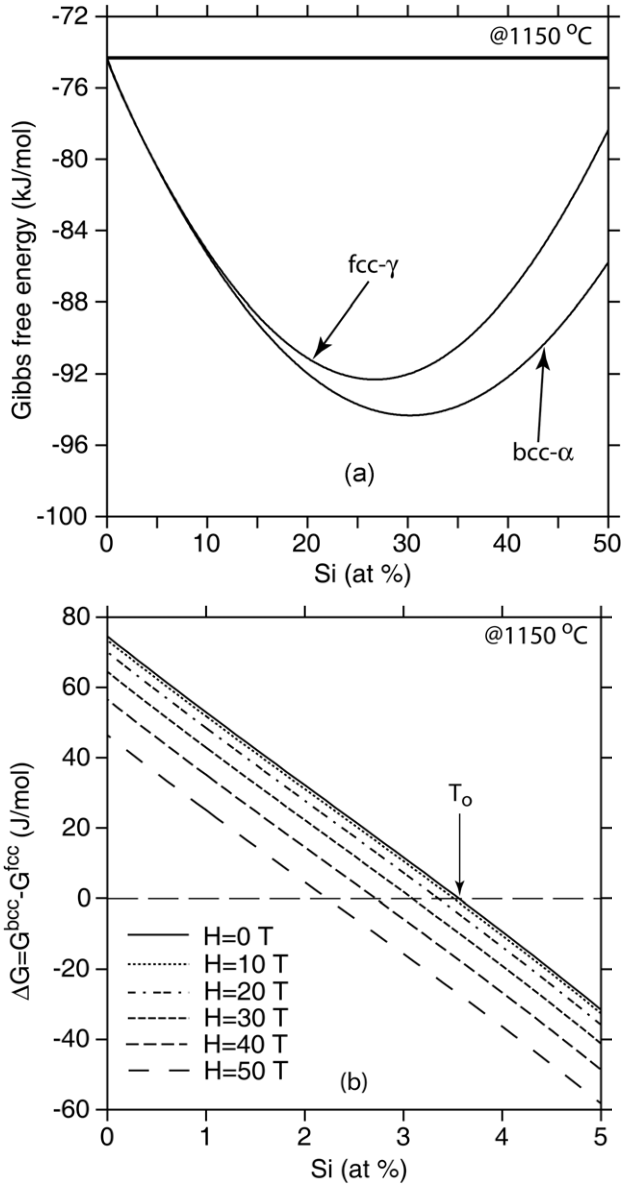

Figure 2. (*a*) The Gibbs energy-composition plot of solid solution α (bcc_A2) and γ (fcc_A1) phases in the Fe–Si system at 1150 °C without external magnetic field, using the thermodynamic database [35]. Since their Gibbs energies are similar for the same composition in the Fe-rich side, the 2-phase field of α and β phases spans a very narrow composition range (see figure 1). (*b*) The Gibbs energy difference between in α and γ phases with varying field strength at 1150 °C. As increasing field strength, the α phase becomes progressively more stable than the γ phase. The arrow marks the T_0 point.

2. Thermodynamic models

In the framework of the CALPHAD method, the Gibbs energy of individual phases without an applied external (magnetic or electrical) field is described by sublattice models [29, 30] and is defined relative to the stable element reference (SER), i.e. the enthalpies of the pure elements in their defined reference

phase at 298.15 K and 1 atm. For example, the total Gibbs energy of a solid solution ϕ phase in the Fe–Si system without an external field consists of two parts, namely, the contribution from the non-magnetic state ($\Delta G^{\text{non-mag}}$, the sum of the first 3 terms in equation (1)) and from the internal magnetic state ($\Delta G^{\text{mag}}_{\text{int}}$), the 4th term in equation (1)) where it cannot be ignored (e.g. ferromagnetic, antiferromagentic and paramagnetic materials):

$$G^{\phi}_{\text{Fe,Si}} = \sum_{i=\text{Fe,Si}} x_i {}^{\text{o}}G^{\phi}_i + RT \sum_{i=\text{Fe,Si}} x_i \ln x_i + {}^{\text{ex}}G^{\phi}_{\text{Fe,Si}} + {}^{\text{mag}}G^{\phi}_{\text{int}}. \tag{1}$$

where ${}^{\text{o}}G^{\phi}_i$ is the molar Gibbs energy of the pure element i in the structure of phase ϕ in the non-magnetic state, taken from the values tabulated by Dinsdale [31], and x_i is the mole fraction of each component. The excess Gibbs energy ${}^{\text{ex}}G^{\phi}_{\text{Fe,Si}}$ is expressed in Redlich–Kister polynomial form [32]

$${}^{\text{ex}}G^{\phi}_{\text{Fe,Si}} = x_{\text{Fe}}x_{\text{Si}} \sum_{k=0}^{k} {}^{k}L^{\phi}_{\text{Fe,Si}}(x_{\text{Fe}} - x_{\text{Si}})^k, \tag{2}$$

where ${}^{k}L^{\phi}_{\text{Fe,Si}}$ are the binary interaction parameters and are typically modelled as

$${}^{k}L^{\phi}_{\text{Fe,Si}} = {}^{k}a + {}^{k}bT + {}^{k}cT\ln(T) + \cdots. \tag{3}$$

The internal magnetic contribution to the Gibbs energy (${}^{\text{mag}}G^{\phi}_{\text{int}}$) without an applied external field is described in [33, 34] as

$${}^{\text{mag}}G^{\phi}_{\text{int}} = RT\ln(\beta + 1)f(\tau), \tag{4}$$

where β is the Bohr magnetic moment per mole of atoms, $\tau = T/T_{\text{C}}$ and T_{C} is defined as the critical temperature for magnetic ordering (i.e. the Curie or Néel temperature). $f(\tau)$ is a polynomial function given in [34]. For solid solution phase ϕ (e.g. the fcc or bcc phase in the Fe–Si system), both T_{C} and β are composition dependent:

$$T^{\phi}_{\text{C}} = \sum_{i=\text{Fe,Si}} x_i T_{\text{C}i} + x_{\text{Fe}}x_{\text{Si}} \sum_{k=0}^{k} {}^{k}T_{\text{CFe,Si}}(x_{\text{Fe}} - x_{\text{Si}})^k, \tag{5}$$

$$\beta^{\phi} = \sum_{i=\text{Fe,Si}} x_i \beta_i + x_{\text{Fe}}x_{\text{Si}} \sum_{k=0}^{k} {}^{k}\beta_{\text{Fe,Si}}(x_{\text{Fe}} - x_{\text{Si}})^k, \tag{6}$$

where $T_{\text{C}i}$ and β_i are the corresponding parameters of the pure elements, and $T_{\text{CFe,Si}}$ and $\beta_{\text{Fe,Si}}$ are the binary magnetic interaction parameters. The Fe–Si binary system was assessed thermodynamically by Lacques and Sundman [35], and their assessed thermodynamic descriptions without an applied external field were adopted directly in the current study.

When an external magnetic field is applied, there is an additional contribution to the total Gibbs energy of the ϕ phase, $\Delta G^{\text{mag}}_{\text{ext}}$, and the total Gibbs energy for the ϕ phase becomes

$$G_{\text{tot}} = \Delta G^{\text{non-mag}} + \Delta G^{\text{mag}}_{\text{int}} + \Delta G^{\text{mag}}_{\text{ext}}. \tag{7}$$

If it is assumed that $\Delta G^{\text{non-mag}}$ and $\Delta G^{\text{mag}}_{\text{int}}$ are not affected significantly by the field, then they can be taken directly from the available thermodynamic databases without modification. Therefore, the key is to determine $\Delta G^{\text{mag}}_{\text{ext}}$

$$\Delta G^{\text{mag}}_{\text{ext}} = -\mu_0 \int_0^H M\,\text{d}H. \tag{8}$$

Here, M is the magnetization, H is the applied field strength and μ_0 is the vacuum permeability (depending on the units used for M and H μ_0 may or may not appear in equation (8)). When the applied field strength is small, M and H obey a linear relationship in χ, the magnetic susceptibility

$$M = \chi H. \tag{9}$$

If the material of interest is paramagnetic and obeys the Curie–Weiss law [36], then χ can be determined as

$$\chi = C/(T - \theta_{\text{c}}), \tag{10}$$

where, C is the Curie–Weiss constant [36]; θ_{c} is a paramagnetic/asymptotic Curie temperature constant, both dependent on alloy composition for a solution phase [36]. Pure Fe [21–27], Fe–Si alloys [21] and many other paramagnetic materials [36] have been reported to obey the Curie–Weiss law in their paramagnetic state (also shown in figure 3 in this report). Therefore, for cases where the magnetic susceptibility does not vary significantly with applied field strength so that the Curie–Weiss law is still valid, the contribution to the Gibbs energy from applied field can be computed by substituting equation (9) into equation (8) and then performing the integration

$$\Delta G^{\text{mag}}_{\text{ext}} = -\frac{1}{2}\mu_0 \chi H^2. \tag{11}$$

3. Results and discussion

Since the bcc-Fe, fcc-Fe and bcc Fe–Si alloys of interest all obey the Curie–Weiss law [21–27], $\Delta G^{\text{mag}}_{\text{ext}}$ can be calculated directly from equation (11) provided that the law is still valid under the applied field. Since a set of reasonable values of the susceptibility for pure Fe is critical to the value of $\Delta G^{\text{mag}}_{\text{ext}}$ of Fe and Fe–Si systems and there are more reported values for pure Fe than evaluated in [21], it is necessary to re-evaluate these values. Figure 3 plots the inverse value of paramagnetic susceptibility of α-, γ- and δ-Fe as a function of temperature. The values for α-Fe appear to be very consistent, but the scatter in the values for γ-Fe and δ-Fe is apparent (especially for γ-Fe). The commonly accepted relationship for α-Fe [21, 22] was originally reviewed in [21] as follows:

$$\chi^{\alpha} = \frac{2.2 \times 10^{-2}}{T - 1093}[\text{cm}^3\,\text{g}^{-1}] \tag{12}$$

However, the values used in equation (12) is not in good agreement with experimental data for α-Fe (see the dashed line in figure 3), although it agrees well with the experimental data for δ-Fe reported by Sucksmith and Pearce [25]. Further, equation (12) predicts that the susceptibility goes to zero at $T = 820\,^{\circ}\text{C}$ whereas the experimental value is 9.52×10^{-4} [cm^3 g^{-1}] [21] at that temperature. Since both α- and δ-Fe have the same bcc crystal structure and both obey the Curie–Weiss law, it is reasonable to assume that both should have the same values of C and θ_{c}, since they are essentially the same phase. Therefore, it is reasonable to enquire whether the poor agreement of equation (12) with experimental values of χ for α-Fe is due solely to inaccurate linear regression treatment, especially considering that there were few reports

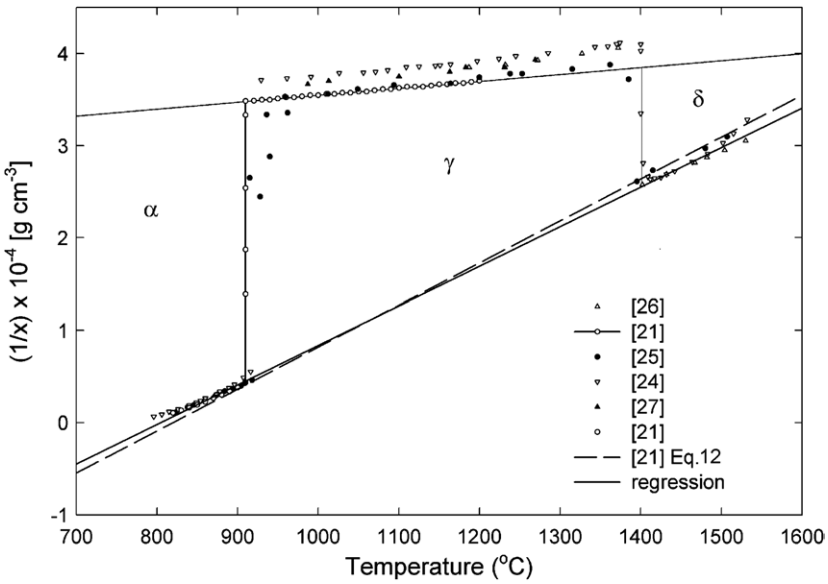

Figure 3. The inverse paramagnetic susceptibility of bcc (α and δ) and fcc (γ) Fe [21–27]. The dashed line represents the regression line evaluated by Arajs and Miller [21] and [22] (also shown in equation (12) in this report for convenience). The solid regression lines are for bcc and fcc Fe re-evaluated in this study.

on the susceptibility of δ-Fe when [21] was written. Since Arajs and Miller used zone-refined Fe with ultra high purity, they determined that the α/γ transition occurs at 910 °C and their susceptibility data appear to be self consistent (figure 3). Therefore, their data set was used to re-evaluate the values of C and θ_c for bcc-Fe (α- and δ-Fe) together with the susceptibility data of Terry [24] and Briane [26]. The values in the vicinity of the α/γ-Fe phase transition and at $T \leqslant 820$ °C were not used, because the former may not be reliable due to the allotropic phase transformation and the latter starts to deviate from the Curie–Weiss law. The re-evaluated susceptibility for bcc-Fe is given in equation (13) (see the regression line in figure 3):

$$\chi^{\alpha} = \frac{2.33 \times 10^{-2}}{T - 1078}\ [\mathrm{cm^3 g^{-1}}] \tag{13}$$

Note that equation (13) is only valid when $T > 1084$ K, since for temperatures close to (i.e. $T - T_c \lesssim 40$ K) the ferromagnetic Curie temperature, 1044.1 K, the paramagnetic susceptibility deviates from the Curie–Weiss law as shown in equation (14) [23]:

$$\chi^{\alpha} = K\,(T - 1044.1)^{-1.33}\ [\mathrm{cm^3\,g^{-1}}] \tag{14}$$

The values of C and θ_c for γ-Fe are not reported in [21, 22]. In this study they were obtained by linear regression on the susceptibility data of γ-Fe measured by Arajs and Miller [21]:

$$\chi^{\gamma} = \frac{1.33 \times 10^{-1}}{T + 3451}\ [\mathrm{cm^3\,g^{-1}}] \tag{15}$$

Both C and θ_c for bcc Fe–Si alloys depend on the Si content, but their compositional dependence is rather weak at low Si contents ($\leqslant$5.57 at.%) [21]. The Thermo-Calc^{TM} package does not currently allow a user to introduce an extra contribution to the Gibbs free energy that varies with composition into the GES module and subsequently compute phase equilibria to map out a new phase diagram in the POLY3 module; such a capability would require modification of its core program codes [37].[4] Therefore, the compositional dependence of the susceptibility was ignored in this study. In fact, the γ phase in interest has a maximum solubility of <4 at.% Si without applied field. However, it must be pointed that in order to compute the other phase boundaries such as α-Fe–Si/α_2/α_1/Fe_5Si_3 etc the compositional dependence must be taken into account because it is too significant to be ignored. With this simplification, the change in Gibbs free energy due to applied field in pure Fe in the paramagnetic state at $T \geqslant 1084$ K is calculated from equations (16)[5] and (17):

$$\Delta G^{\alpha}_{\mathrm{ext}} = -\frac{1.0293 \times 10^{-11}}{T - 1078} H^2\ [\mathrm{J\,mol^{-1}}] \tag{16}$$

$$\Delta G^{\gamma}_{\mathrm{ext}} = -\frac{5.8735 \times 10^{-11}}{T + 3451} H^2\ [\mathrm{J\,mol^{-1}}]. \tag{17}$$

The calculated Gibbs energy change due to applied field of $H = 15$, 30 and 50 T for α and γ Fe are illustrated figure 4. As expected, it is always significantly more negative for the bcc-Fe than for the fcc-Fe; thus the external magnetic energy to the α phase dominates the phase relations with field. The external magnetic energy is significant at relatively low temperatures for the α phase and then levels off steadily with rising temperature. The temperature effect on paramagnetic fcc-Fe is negligible since it follows a linear relationship for varying field strength.

The effect of the applied field on the allotropic α/γ-Fe transition is shown in figure 5(a), and only the Gibbs energy difference between bcc (α and δ) and fcc (γ)-Fe is plotted instead of their individual values which are too close to be distinguished. The location of the invariant $\alpha \leftrightarrow \gamma$ transition temperature was determined from the zero point of

[4] More details about GES and POLY3 modules can be found in the User's Guide of Thermo-Calc^{TM}. It can be downloaded from www.thermocalc.com.
[5] Field strength: 1[T] = 10^4 [Oe] = 7.958×10^5 [Am^{-1}]. Mass susceptibility: 1 cm^3 g^{-1} [CGS] = $4\pi \times 10^{-3}$ m^3 kg^{-1} [ISO].

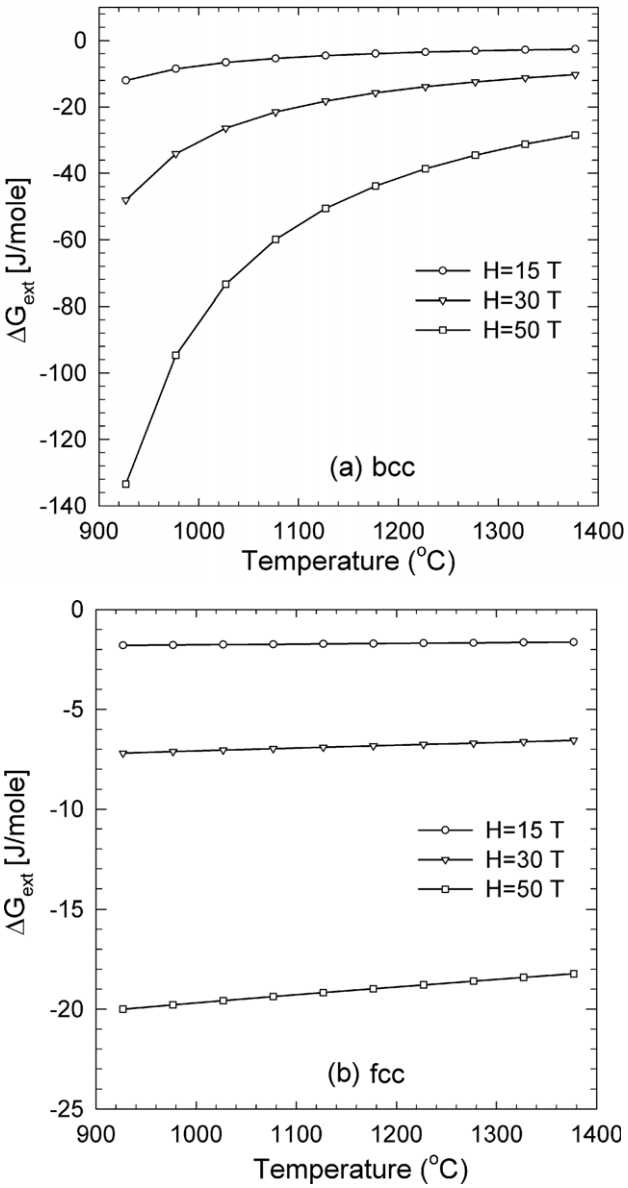

Figure 4. External magnetic energy to (*a*) bcc-α and (*b*) fcc-γ phases of pure Fe with varying field strength.

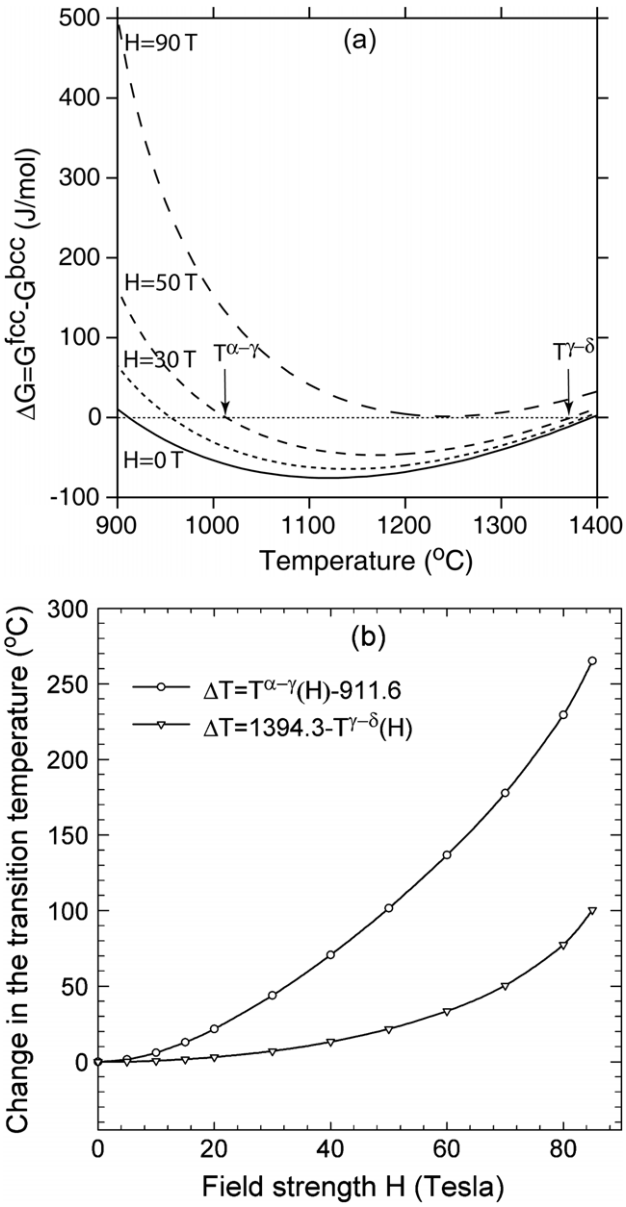

Figure 5. (*a*) Change in molar Gibbs energy difference (i.e. $\Delta G^{\text{fcc–bcc}}$) between bcc-Fe and fcc-Fe, versus temperature with varying field strength of $H = 0$, 30, 50 and 90 T. The temperature of the polymorphous transitions of $\alpha \leftrightarrow \gamma$ and $\gamma \leftrightarrow \delta$ is defined by the arrows where $\Delta G = G^{\text{fcc}} - G^{\text{fcc}} = 0$ (note $\mu^{\phi} = G^{\phi}$ for a single-component system). Note that fcc-Fe eventually becomes unstable when a hypothetical strength of $H = 90$ T is applied. (*b*) Change in the bcc–fcc transition temperature of Fe due to applied field.

the energy difference. The calculated invariant temperature of the allotropic bcc↔fcc transitions versus field strength is listed in table 1 and also plotted in figure 5(*b*). The hypothetical field strength (>50 T) is included in the plots to show the general trend. The calculated invariant temperatures are all smaller than previously calculated values for respective field strength [7–9, 13]. The reasons for the difference are a consequence of (1) current report used experimentally determined values of susceptibility of α-Fe; (2) the fact that Enomoto *et al* [9] ignored the effect of external field on the γ-Fe; (3) Enomoto *et al* [9] and Joo [7, 13] used a more simplified thermal energy description for pure Fe.

The calculated Gibbs energy (including $\Delta G^{\text{non-mag}}$, $\Delta G^{\text{mag}}_{\text{int}}$ and $\Delta G^{\text{mag}}_{\text{ext}}$) difference between the bcc and fcc phases in Fe–Si system is shown in figure 2(*b*). With increasing field strength, the bcc phase becomes more stable with respect to the fcc phase and the T_0 point (defined as where their Gibbs energies are equal) is shifted towards Si-poor side. The predicted Fe–Si γ loop with varying field strength is shown in figure 6. As expected, the γ loop shrinks steadily with increasing field strength, but a low field strength $\leqslant$20 T appears to have very small effect on the γ loop. It is not surprising that the effect of the field is more pronounced in the lower temperature portion of the γ loop, and that the change in the α/γ phase transition is much more significant than the γ/δ phase transition of Fe (see figure 6 and also table 1). The γ phase eventually becomes unstable with respect to

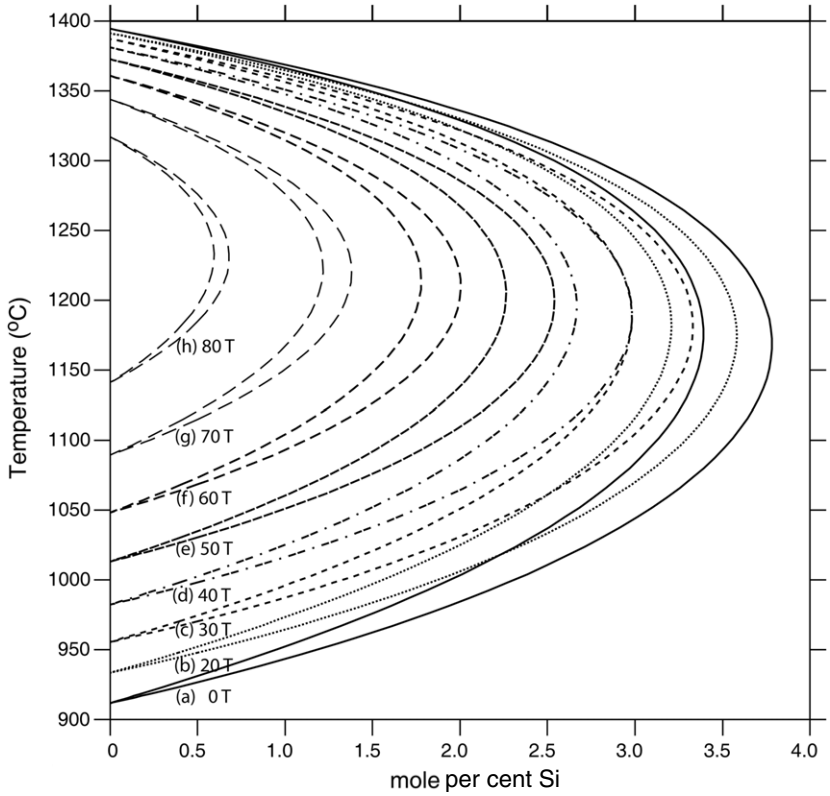

Figure 6. The resulting γ loop in the Fe–Si system with varying field strength of (a) $H = 0$, (b) 20, (c) 30, (d) 40, (e) 50, (f) 60, (g) 70, (h) 80 T, respectively. The γ loop without field is shown as solid curve. As the field strength increases, it shrinks progressively, and its nose is shifted towards higher temperatures and lower Si contents.

Table 1. The bcc–fcc phase transition temperatures in pure Fe with varying field strength, calculated using Thermo-Calc^{TM}. The re-evaluated paramagnetic susceptibility for pure Fe, $\chi^{bcc} = (2.33 \times 10^{-2})/(T - 1078)$ [cm^3 g^{-1}], is used.

Strength (T)	temperature (°C)	
	$T^{\alpha\leftrightarrow\gamma}$	$T^{\gamma\leftrightarrow\delta}$
0	912	1394
5	913	1394
10	918	1394
15	925	1393
20	933	1391
30	956	1387
40	982	1381
50	1013	1373
60	1048	1361
70	1089	1344
80	1141	1317
85	1177	1294

the α phase (as a function of temperature and Si contents) when a hypothetically high field of $H \geqslant 85$ T is applied, and then an Fe–Si electrical steel would 'virtually' experience no phase transformations at all during thermo-mechanical processing assisted by magnetic field. A previous report [8] predicted that γ-Fe becomes unstable with respect to α-Fe at any temperatures with a high field $\geqslant$100 T, but this is likely an overestimation of the effect of the field due to the reasons aforementioned.

As magnetic thermo-mechanical processing emerges as a novel tool for inventing new classes of materials of superior properties, the capability of predicting the changes in alloy phase diagrams under external magnetic field becomes very important for the design of alloys and their processing. The effect of applied magnetic fields on the stability of the γ loop in Fe–Si system appears not to be significant up to a field strength of 50 T because the competing phases of both bcc and fcc solid solution are all paramagnetic. However, the situation would be very different when the system of interest could involve a ferromagnetic phase ($T \leqslant T_c$, the ferromagnetic Curie temperature); again, the phase boundaries can be shifted significantly [1, 4–7, 12, 13, 16, 19, 20] but additional evaluation of Gibbs energy changes under applied field would have to be performed. Also, the phase transformation kinetics can be affected significantly because of the changes in driving forces and atomic diffusivities [14, 19]. Therefore, it is important to develop computational tools to predict phase stability under external magnetic fields and to be able to compute phase diagrams. In order to do so, the first step is to develop a constitutive equation involving magnetization with applied field that is appropriate for incorporation into the current CALPHAD methodology for rapidly optimizing phase thermodynamic parameters with reasonable accuracy, covering the whole temperature range (i.e. from room temperature to the liquid phase). An immediately available equation is Weiss molecular field theory (WMF) that describes magnetization response with applied

field through the Brillouin function [see [9, 13, 36] for details]. A direct comparison between WMF prediction and experiments is rare because so few experiments have been performed. Recently, however, Hao and Ohtsuka reported that the WMF theory underestimates the magnetization of Fe–C alloys [12]. Therefore a comprehensive examination on WMF predictions should be made before it is developed to calculate phase diagrams with applied field.

However, when the system concerned is paramagnetic (the temperature concerned is well above the critical ordering temperature, ferromagnetic Curie temperature for ferromagnetic materials, Néel temperature for antiferromagnetic materials) and the materials obey the Curie–Weiss law, then the computation of phase equilibria with applied field becomes more straightforward. The change in the Gibbs energy due to the field can be directly determined via equation (8). Although some experimental susceptibility data may be available, its compositional dependence must be taken into account. This can be done through an optimization scheme in the CALPHAD calculation engine (e.g. PARROT module) to quantify a set of parameters to describe the compositional dependence of the Curie constant C and the temperature constant θ_c. Specifically, the current authors proposed that C and θ_c can be modelled in the Redlich–Kister polynomial form [32] for an A–B binary system:

$$C = \sum_{i=A,B} x_i {}^{o}C_i + x_A x_B \sum_{i=0}^{k} {}^{k}C_{A,B}(x_A - x_B)^k \qquad (18)$$

$$\theta_c = \sum_{i=A}^{B} x_i {}^{o}\theta_{c(i)} + x_A x_B \sum_{i=0}^{k} {}^{k}\theta_{c(A,B)}(x_A - x_B)^k. \qquad (19)$$

Here ${}^{o}C_i$ is the Curie–Weiss constant for the pure component i in the ϕ phase, and ${}^{k}C_{A,B}$ is the interaction parameter of order k ($\geqslant 0$) for the same ϕ phase of components A and B for the Curie constant. ${}^{o}\theta_{c(i)}$ is the paramagnetic/asymptotic Curie temperature constant (in K) of the ϕ phase of pure component i, and ${}^{k}\theta_{c(A,B)}$ is the interaction parameter of order k ($\geqslant 0$) for the same ϕ phase of components A and B for the critical temperature. x_A and x_B are the mole fractions of components A and B, respectively, in the ϕ phase.

4. Conclusions

We have applied the CALPHAD method to investigate the effect of an external magnetic field on the Fe-rich Fe–Si system based on the Curie–Weiss law and re-evaluated susceptibility data [21–27]. A set of CALPHAD-consistent thermodynamic descriptions for pure Fe with an applied field was developed in the paramagnetic state. The calculated invariant temperatures of bcc–fcc allotropic transformations with an applied field are all smaller than previously calculated values for respective field strength [7–9, 13]. The present results are more accurate because current report used (1) better values of susceptibility of Fe and (2) more robust computational tools. Finally, a CALPHAD compatible model to reflect the compositional dependence of the Curie–Weiss law is proposed in order to combine external magnetic energy into well-developed CALPHAD methodology [28].

Acknowledgments

MCG and ADR acknowledge financial support from the Computational Materials Science Network, a program of the Office of Science, US Department of Energy. MCG thanks Q Chen for help with figure 2(*b*). Useful discussions with Thermo-Calc Software Inc. staff including P Mason, Q Chen and A Engström on the possibility to link Thermo-Calc™ with external magnetic energy is acknowledged.

References

[1] Shimizu K and Kakeshita T 1989 *ISIJ Int.* **29** 97–116
[2] Molodov D A, Gottstein G, Heringhaus F and Shvindlerman L S 1998 *Acta Mater.* **46** 5627–32
[3] de Oliveira N A 2003 *J. Phys. Chem. Solids* **64** 1173–7
[4] Kakeshita T, Sato Y, Saburi T, Shimizu K, Matsuoka Y and Kindo K 1999 *Mater. Trans. JIM* **40** 100–6
[5] Koch C C 2000 *Mat. Sci. Eng.* A **287** 213–18
[6] Choi J K, Ohtsuka H, Xu Y and Choo W Y 2000 *Scr. Mater.* **43** 221–6
[7] Joo H D, Kim S U, Shin N S and Koo Y M 2000 *Mater. Lett.* **43** 225–9
[8] Guo H and Enomoto M 2000 *Mater. Trans. JIM* **41** 911–16
[9] Enomoto M, Guo H, Tazuke Y, Abe Y R and Shimotomai M 2001 *Metall. Mater. Trans.* A **32** 445–53
[10] Sheiko L, Sadovoy A, Troschenkov Y and Kulyk O 2002 *J. Phys. D: Appl. Phys.* **35** 1765–7
[11] Shimotomai M, Maruta K, Mine K and Matsui M 2003 *Acta Mater.* **51** 2921–32
[12] Hao X and Ohtsuka H 2004 *Mater. Trans. JIM* **45** 2622–5
[13] Joo H D, Choi J K, Kim S U, Shin N S and Koo Y M 2004 *Metall. Mater. Trans.* A **35** 1663–8
[14] Yang J and Goldstein J I 2004 *Metall. Mater. Trans.* A **35** 1681–90
[15] Nicholson D M C *et al* 2004 *J. Appl. Phys.* **95** 6580–2
[16] Zhang Y, Gey N, He C, Zhao X, Zuo L and Esling C 2004 *Acta Mater.* **52** 3467–74
[17] Molodov D A and Sheikh-Ali A D 2004 *Acta Mater.* **52** 4377–83
[18] Bennett T A *et al* 2005 *Solid State Phenol.* **105** 151–6
[19] Jaramillo R A *et al* 2005 *Scr. Mater.* **52** 461–6
[20] Zhang Y D, Zhao X A, Bozzolo N, He C S, Zuo L A and Esling C 2005 *ISIJ Int.* **45** 913–17
[21] Arajs S and Miller D S 1960 *J. Appl. Phys.* **31** 986-91
[22] Hellwege K H and Madelung O Landolt-Börstein 1986 *Magnetic Properties of Metals* vol 19 (Berlin: Springer) pp 30–1
[23] Arajs S and Colvin R V 1964 *J. Appl. Phys.* **35** 2424
[24] Terry E M 1917 *Phys. Rev.* **9** 394
[25] Sucksmith W and Pearce R R 1938 *Proc. R Soc. Lond.* A **167** 189–204
[26] Briane M 1972 *C. R. Acad. Sci. Ser.* B **275** 673
[27] Nakagawa Y 1956 *J. Phys. Soc. Japan* **11** 855
[28] Sundman B, Jansson B and Andersson J O 1985 *CALPHAD* **9** 153–90
[29] Hillert M and Staffanson L I 1970 *Acta Chem. Scand.* **24** 3618–26
[30] Hillert M 2001 *J. Alloys Compounds* **320** 161–76
[31] Dinsdale A T 1991 *CALPHAD* **15** 317–425
[32] Redlich O and Kister A T 1948 *Ind. Eng. Chem.* **40** 345
[33] Inden G. *Proc. Project Meeting CALPHAD V (Düsseldorf, 1976)* p III.4.1
[34] Hillert M and Jarl M 1978 *CALPHAD* **2** 227
[35] Lacques L and Sundman B 1990 *Metall. Mater. Trans.* A **22** 2211–23
[36] Jiles D 1991 *Introduction to Magnetism and Magnetic Materials* (London: Chapman and Hall)
[37] Chen Q, Mason P and Engström A private communication, Thermo-Calc Software Inc